Hindawi
Indoor Air
Volume 2024, Article ID 5055615, 14 pages
https://doi.org/10.1155/2024/5055615

Research Article

Development of Particle Filters for Portable Air Purifiers by Combining Melt-Blown and Polytetrafluoroethylene to Improve Durability and Performance

Hyunjun Yun,[1] **Ji Hoon Seo**,[2] **and Jinho Yang**[3]

[1]*The AI Convergence Appliance Research Center, Korea Electronics Technology Institute, 226 Cheomdangwagi-ro, Buk-gu, Gwangju 61011, Republic of Korea*
[2]*Department of Environmental Health, Korea University, 145, Anam-ro, Seongbuk-gu, Seoul 02841, Republic of Korea*
[3]*Department of Occupational Health and Safety, Semyung University, 65 Semyung-ro, Jecheon, Chungcheongbuk-do 27136, Republic of Korea*

Correspondence should be addressed to Jinho Yang; iamjinho@semyung.ac.kr

Received 7 November 2023; Revised 20 March 2024; Accepted 1 April 2024; Published 24 April 2024

Academic Editor: Xiaohu Yang

Improving indoor air quality through the use of air purifiers has become a major focus, with emphasis on developing filters with high efficiency, high holding capacity, and low-pressure drop to improve the clean air delivery rate (CADR) for air purifiers. However, although most studies focused on developing media and evaluating their performance, few studies have reached the employment for a pleated filter. In this study, we newly synthesized flat media and pleated filters by combining polytetrafluoroethylene membrane (PT) and melt-blown (MB) materials (PM) and compared its initial performance to that of other air purifier filters (MB, glass fiber, and PT). Additionally, we analyzed how the performance changed after the particles were loaded. The initial efficiency of the PM filter showed a higher quality factor (QF) than the other filters. Furthermore, when more particles were loaded, the penetration of the PM did not change. These results demonstrate the potential of the PM. However, the CADR and submicron-sized (0.02–0.113 μm) CADR (sCADR) were highest for the MB filter due to the initial pressure drop. Therefore, additional improvements are required to apply the PM in air purifiers. However, the results suggest that the PM can be a new alternative for air purifier filters used in medical centers or facilities with vulnerable populations where a high-efficiency particle air (HEPA) filter must be used.

1. Introduction

East Asian countries, including China, face immense challenges due to the recent increase in submicron particle (0.02–0.113 μm) concentrations associated with rapid industrialization [1, 2]. These submicron particles are mainly attributable to the burning of gasoline and diesel fuel, black carbon, tobacco, photochemical reactions, and oil particles released by cooking. The indoor submicron particle concentration is also influenced by the infiltration of submicron particles of an outdoor origin into the indoor environment [3]. High concentrations of submicron particles are a health risk factor and a threat to the environment [4–7]. In addition, harmful microbes, including bacteria, fungi, and viruses such as SARS-CoV-2, MERS-CoV, and SARS-CoV-1, have been reported as submicron particles [4, 8–10].

To curb indoor submicron particle concentration effects, the use of air purifiers has gained popularity in both residential and commercial spaces [4]. Several studies have demonstrated that air purifiers are an efficient method for improving indoor air quality. A portable high-efficiency filter can be used as a treatment for patients with asthma [11]. In addition, previous studies have reported significant improvement in some allergy symptoms through the use of a high-performance air purifier [12, 13]. However, several inefficient air purification systems have penetrated the market, highlighting the need to evaluate the quality of air purifier systems. In addition, understanding of air purifier performance is affected by a lack of real-use

experiments. Currently, the performance of air purifiers is not measured in end-user settings. Each air purifier is tested for its clean air delivery rate (CADR) in testing chambers in each country according to its own standards, such as ANSI/AHAM AC-1-2006 [14], GB/T18801-2015 [15], and SPS-KACA002-132 [16], and the size and range of particles are defined differently in each country.

The performance of an air purifier is primarily determined by the type and quality of the filter. Filters fall into two popular categories: fiber filters and membrane filters [5]. Air purifiers with high-efficiency particulate air (HEPA) filters have gained popularity because of their simplicity and high efficiency [5, 7, 17, 18]. However, many commercial air purifiers that work in the same way as HEPA units but are so-called HEPA-type electret fiber filters (e.g., charged melt-blown (MB) filters), do not comply with the same standards [4]. Although HEPA-type filters have a high CADR, their collection efficiency decreases sharply as particles are loaded into the filter fibers [19–21]. This may be attributable to fiber charge neutralization, filter charge screening, and chemical interactions between the aerosols and the filter material [19, 21]. In contrast, membrane filters generally have a relatively high solid fraction, which provides high efficiency [5, 22–24]. However, particles larger than a regular void space may cause a drastic pressure drop, leading to a greater dependence on surface filtration than depth filtration [5, 25]. Although filters are a key determinant of air purifier efficiency and provide an opportunity for performance improvement, studies on the efficiency of air purifiers with different filter types are limited.

This study is aimed at developing a filter with an optimized combination medium to achieve low differential pressure and an extended lifespan. Such efforts would help overcome the problem of rapid performance deterioration experienced with conventional charged MB filters and extend the replacement cycle of filters, thereby mitigating environmental pollution caused by filters. To assess the performance of the filter we developed, we conducted a comparative evaluation with existing filters, including charged MB, glass fiber, and polytetrafluoroethylene (PTFE) filters. Additionally, we aimed to evaluate any performance differences of the new filter before and after particle loading, comparing it with existing filters manufactured in this study. These filters were subsequently installed in identical commercial air cleaners to investigate their impact on the air cleaner's CADR, emphasizing the critical necessity for efficient air purification systems in the current market. These results are expected to serve as a foundation for providing filters that implement space-specific optimized performance in existing air purifiers, thereby laying the groundwork for providing occupants with safe and comfortable air, countering the indiscriminate use of existing air purifiers.

2. Methods

2.1. Flat Media and Pleated Filter Specifications. The specifications of the flat filter media, that is, the charged melt-blown (MB), glass fiber (GF), PTFE membrane (PT), and PTFE-MB combined media (PM), are listed in Table S1. The GF, MB, and PT filters are commercially available. The modified composite media was coupled to a spun bond ($30\,g/m^2$) material on both sides of the PTFE membrane, and a further charged MB ($20\,g/m^2$) layer was designed to bind to one side of the outer surface. The PTFE manufacturing process and the lamination process are shown in Figure 1. The flat media test was conducted according to the modified US 42 CFR Part 84 [26]. US 42 CFR Part 84 is one of the regulations provided by the Centers for Disease Control and Prevention (CDC) in the United States, encompassing aerosol filtration efficiency, pressure drop, and user comfort for respiratory masks made of fibrous filter materials [27, 28]. At a face velocity of 5 cm/s, the particle removal efficiency determined using an automated filter tester (model 8130, TSI, Inc., Shoreview, MN, USA) of all the media used in this experiment was more than 99.95%. The percentage of particle penetration and pressure drop were measured at a flow rate of 32 L/min using a NaCl aerosol. Five samples of each flat filter medium were tested for particle penetration. For all types of media (MB, GF, PT, and PM), we produced a pleated filter with a size of 277 mm × 361 mm × 35 mm and area of $1.84\,m^2$, as shown in Figure 2.

2.2. Measurement of Initial Filter Penetration and Differential Pressure. Filter penetration and pressure drop were measured using the cabin air filter test system PAF-111 (Topas GmbH, Dresden, Germany). The experimental system and procedures were in accordance with ISO 11155-1, which is the standard for automotive passenger seat filters [29]. The experimental apparatus was a modular system. The system was divided into a particle-generator section and a test section. In the particle-generator section, air passes through an EU13 HEPA filter, and then the particles exit the atomizer aerosol generators (model ATM 210, Topas GmbH, Dresden, Germany). The testing was performed using fluid diethylhexyl sebacate (DEHS) particles. In the test section, the upstream and downstream particle removal rates were calculated as the particles passed through the test filter using an optical particle counter (LAP 322, Topas GmbH). The differential pressure drop (ΔP) test measures the ease of air passage through the filter using the upstream-to-downstream pressure drop at a flow rate of 1 m/s. The experiments were repeated three times for each filter.

2.3. Filter Loading Test. The test particles were loaded using the user-defined dust loading test mode of the PAF-111 (Topas GmbH) to determine how the performance changed when particles were loaded into the filter. Many particles found in the environment, such as those produced from cooking, black carbon, oil, and dust, were considered when selecting DEHS (diethylhexyl sebacate) (<1 μm) and ISO 12103-1 A2 dust (0.97–176 μm) as representative test particles for evaluating particle loading [30, 31]. The reason for this selection is that ISO 12103-1 A2 represents coarse particles, while DEHS serves as a surrogate for oil particles. The reason for using standardized particles is that the amount of test dust must be uniform to ensure a constant value of dust concentration. Therefore, it is known that standardized experimental particles should be used in filter

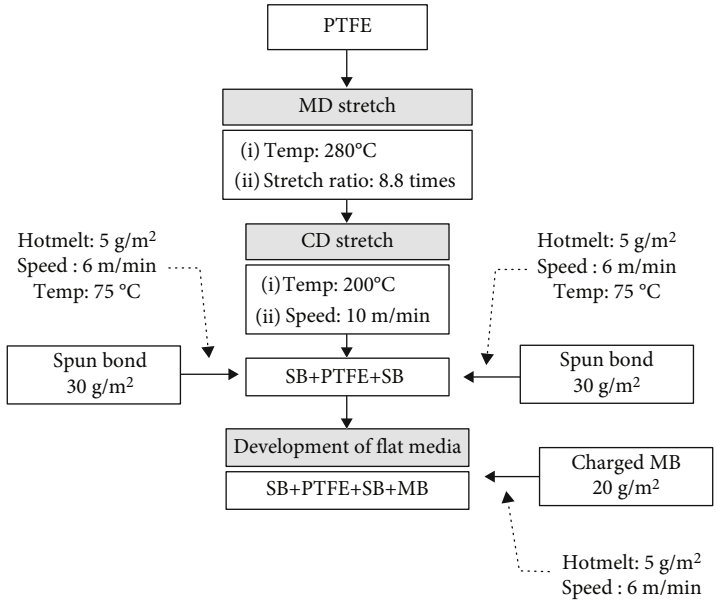

Figure 1: The test bench diagram for development of new flat media.

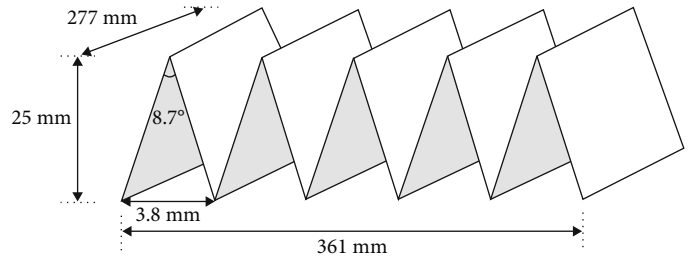

Figure 2: Pleating geometries of pleated filter.

loading tests where reproducibility is required for these reasons [32]. The A2 fine dust was dispersed by dust dispersers (SAG410, Topas GmbH) at 20 g for 30 min, and the solid particles were neutralized using a bipolar aerosol neutralizer unit (EAN 581, Topas GmbH). DEHS particles were obtained from the atomizer aerosol generators (ATM 210, Topas GmbH) and were loaded at a speed of 2 g/30 min. For the particle loading, solid particles were loaded onto the filter, and then liquid particles were loaded. One cycle lasted for 60 min. While the particles were being loaded, the change in the collection efficiency was measured using an optical particle counter (LAP 322, Topas GmbH) upstream and downstream of the test filter. Sensors were used to measure the change in the pressure drop across the filter. The loading experiment was implemented at a flow rate of 200 m^3/h, and the filter performance was evaluated at 0.2, 0.5, and 1.0 m/s. To obtain representative and reliable results, the experiments were repeated three times for each of the four filter media (MB, GF, PT, and PM). The performance and loading test process are shown in Figure 3.

2.4. QF Calculation. To evaluate the change in performance over time based on each filter's features, the quality factor (QF), or figure of merit, an established effective comparison tool for various filter types, was used to compare the performance before and after filter use [33–35]. The QF equation was determined as follows:

$$\mathrm{QF} = \frac{-\ln\left[1 - P\right]}{\Delta P}. \quad (1)$$

Here, P is the particle penetration (fraction of particles passing through a filter) and ΔP is the pressure drop (Pa) of the entire filter. The QF has a higher value when the filter's pressure drop is lower, and vice versa.

2.5. Specifications of the Air Purifiers. A portable air purifier (AP-1018F, Coway Co., LTD, South Korea) (Table S2), which is available in both online and offline stores, was selected for the CADR performance tests of the MB, GF, PM, and PT filters. The filter system was composed of a prefilter, deodorant filter, and particle filter at the time of purchase. The product was certified with a Clean Air Certification from the Korea Air Cleaning Association, and the official CADR result was 4.28 m^3/min. In this study, the prefilter and the experimental filters (MB, GF, PM, and PT) were

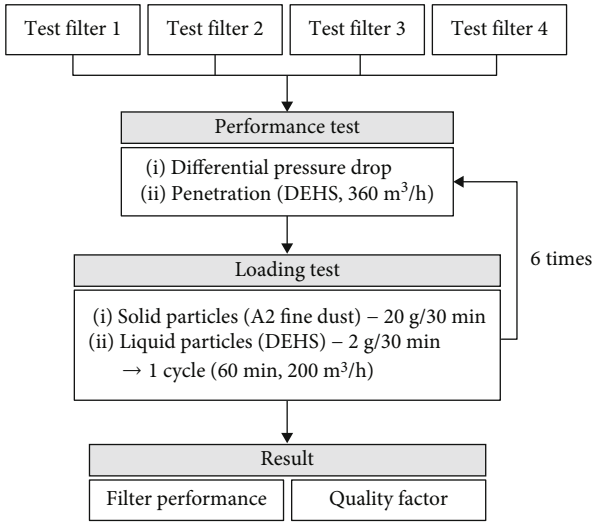

Figure 3: Test bench diagram for performance and loading test process.

used for the tests. From among the four working modes, the CADR tests were conducted in the turbo mode.

2.6. Experimental Measurements. The CADR test was conducted according to the SPS-KACA 002-0132:2018 standard [16] (Figure S1). The performance of an air cleaner is evaluated by its clean air delivery rate (CADR), which is defined as the measure of its delivery of contaminant-free air in cubic meters per minute, with all particles of a given size distribution removed. The chamber size was 30 m^3, following the Korea Air Cleaning Association (KACA) standard (4.0 m (L) × 3.0 m (D) × 2.5 m (H)). The chamber temperature was 23 ± 5°C, and the relative humidity was maintained at 55 ± 15%. Potassium chloride (KCl) was used as the test particle, and its initial particle concentration was 1.0-3.0 × 108 particles/m^3. An aerosol spectrometer (Model 11-A, Grimm Aerosol Technik GmbH & Co. KG, Germany) was used to measure the particles, resulting in a 0.3 μm concentration decay. The sampling interval was one minute. Both natural decay and operational decay tests were conducted for 20 min each or until the concentration reached one-tenth of its initial value. In the operational decay experiment, the first sampling point ($t = 0$) was taken after the air purifier had been running for three minutes.

We measured the submicron (0.02–0.113 μm) CADR (sCADR) to verify the difference in submicron particle removal performance among the filters. When an air purifier's sCADR was measured, submicron KCl particles were created using a nanoparticle generator (EP-NGS20, EcoPictures Co., Ltd., South Korea). Then, the submicron particles were measured using an electrostatic classifier (model 3082, TSI, Inc., Shoreview, MN, USA), an ultrafine condensation particle counter (model 3776, TSI, Inc.), and a differential mobility analyzer (model 3085, TSI, Inc.). The submicron KCl particles were sprayed for 10 min and sampled in 1 min intervals. The natural decay and operational decay were calculated based on SPS-KACA 002-0132:2018. Both CADR and sCADR tests were conducted.

The following equation was used to calculate the purifying capacity (Pc) of the CADR and sCADR:

$$\mathrm{Pc} = \frac{V}{Nt}\left(\ln\frac{C_{i2}}{C_{t2}} - \ln\frac{C_{i1}}{C_{t1}}\right). \quad (2)$$

Here, V is the volume of the chamber, N is the number of experimental air purifiers, C_{i1} is the particle concentration at the beginning of the measurement ($t = 0$) when the capacity decreases naturally, C_{i2} is the particle concentration at the beginning of the measurement ($t = 0$) when the operation decreases, C_{t1} is the particle concentration for each measured t minute when the capacity decreases naturally, and C_{t2} is the particle concentration for each measured t minute when the operation decreases.

The operating electrical power was measured using a digital power analyzer (WR310, Yokogawa Electric Corp., Tokyo, Japan). Before the power measurements, the air purifier was turned to the maximum setting and allowed to operate for 5 min. The power indicator of the digital power analyzer was adjusted to 220 V (60 Hz), and the watt readings were recorded for 10 min at 1 min intervals.

2.7. Statistical Analysis. Regression analysis was performed to determine the correlation between the CADR and energy consumption efficiency, and the correlation coefficient (r) was obtained using SPSS version 22.0 (SPSS Inc., Chicago, IL, USA), where a p value of less than 0.05 was considered statistically significant.

3. Results

3.1. Filter Performance according to Particle Loading by Filter Type. The filter performance and pressure drop varied with the material in Figure 4, and Figure S2 shows the changes in penetration rate and pressure drop after particle exposure. After exposing the filters to DEHS and A2 particles for 30 min each, the pressure drop increased for all filters. The PTFE filter exhibited the highest pressure drop. The MB filter showed an increased penetration rate, but the GF, PM, and PT filters showed decreased rates. The MB filter had the highest initial penetration rate (0.0118) and the lowest pressure drop (68 Pa). The pressure drop increased by 88.2% after 6 cycles of loading at 1 m/s, with a 30% increase in penetration rate (Figure 4(a)). The GF filter had a high initial penetration rate (0.0005) but the highest pressure drop (384 Pa). After six cycles, the pressure drop increased by 26.6% at 1 m/s and the penetration rate decreased by 0.04% (Figure 4(b)). The PM filter had the same initial penetration rate (0.0005) as the GF filter, but it had a lower pressure drop (165 Pa). After six cycles, the pressure drop increased by 91.5% at 1 m/s (Figure 4(c)). The PT filter had an initial penetration rate of 0.001 and an average pressure drop of 210 Pa. After six cycles, the pressure drop increased by 124.2% at 1 m/s and the penetration rate decreased by 0.04%. As the pressure drop of the PT filter increased, the particle removal efficiency also increased (Figure 4(d)).

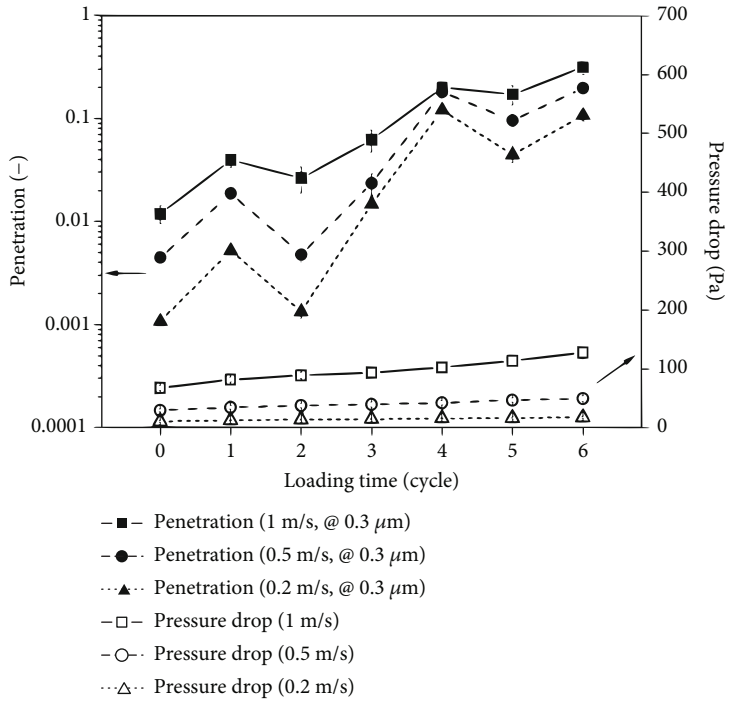

(a)

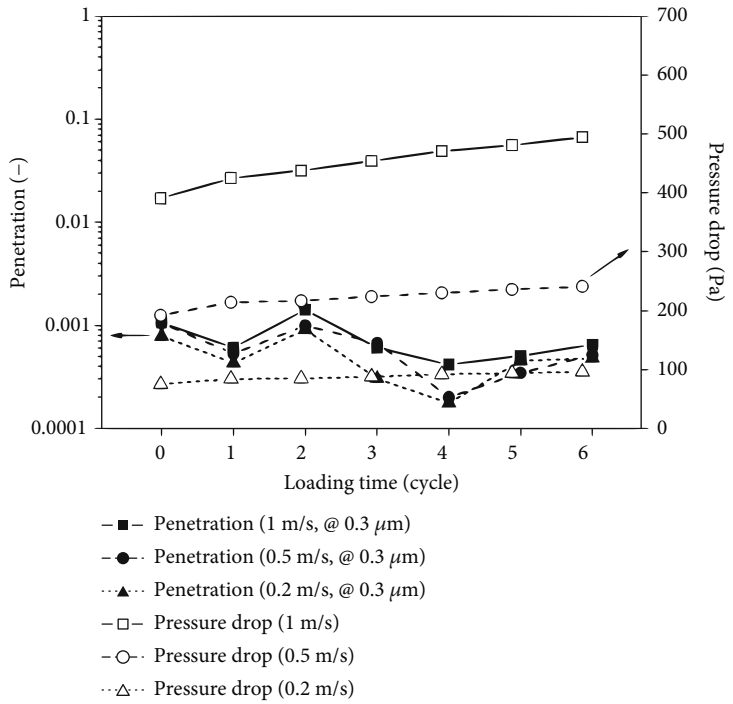

(b)

Figure 4: Continued.

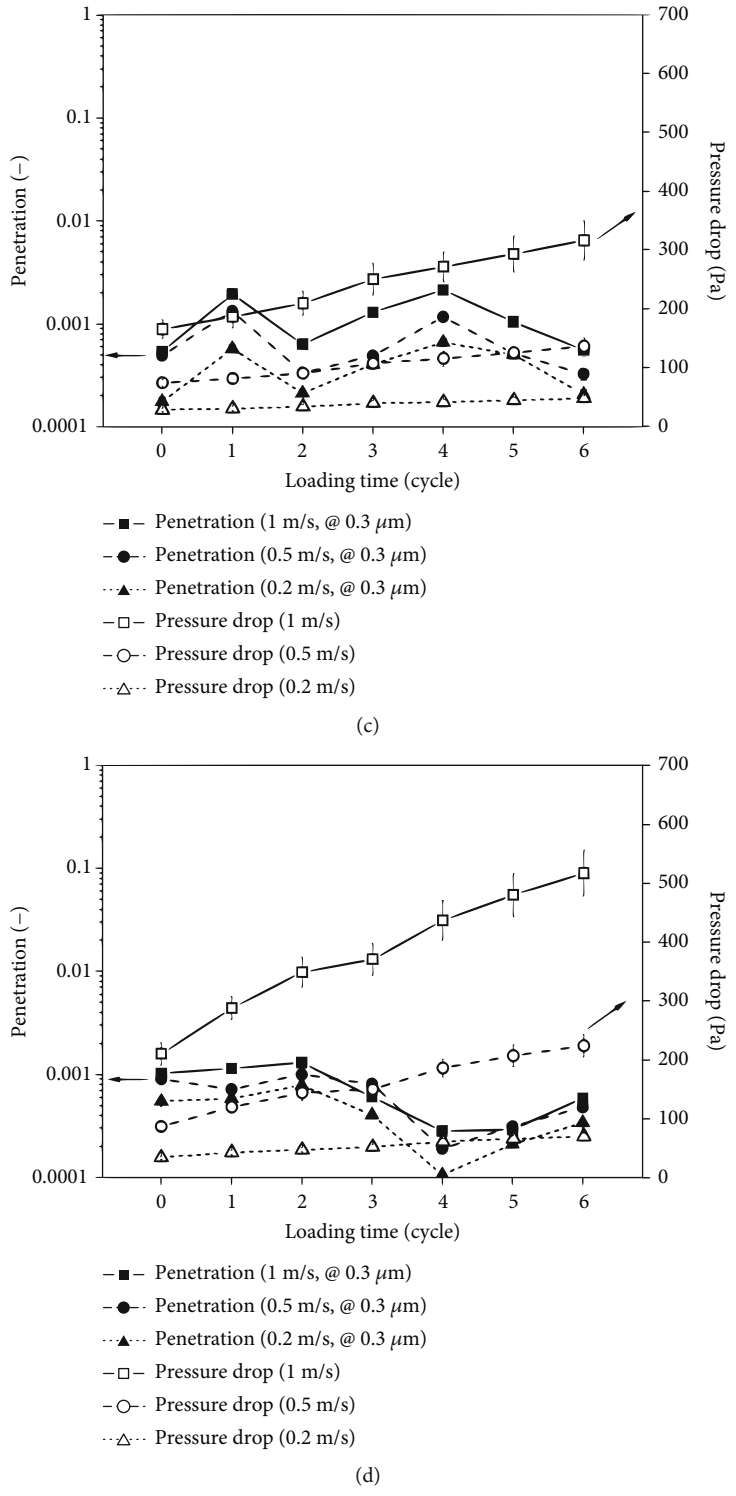

Figure 4: Penetration and pressure drop of the filters loaded with DEHS and A2 as a function of time. (a) Melt-blown (MB) filter, (b) glass fiber (GF) filter, (c) PT + MB (PM) filter, and (d) PTFE membrane (PT).

3.2. QF Performance Test of Filters by Particle Loading Size. Figure 5 illustrates the changes in the performance of each filter as a result of particle loading using the QF values (Table S3). All filters used in the experiment were investigated with the lowest QF values in the range of 0.201–0.245 μm. MB had the highest initial QF value (Figure 5(a)). The QF values were in the same order as the initial measurement results, i.e., MB, PM, PT, and GF, respectively. However, there was a decrease in the particle size range of 0.835–1.17 μm, which had a high QF value of 46.3% for MB, 39.5% for PT, 25.7%

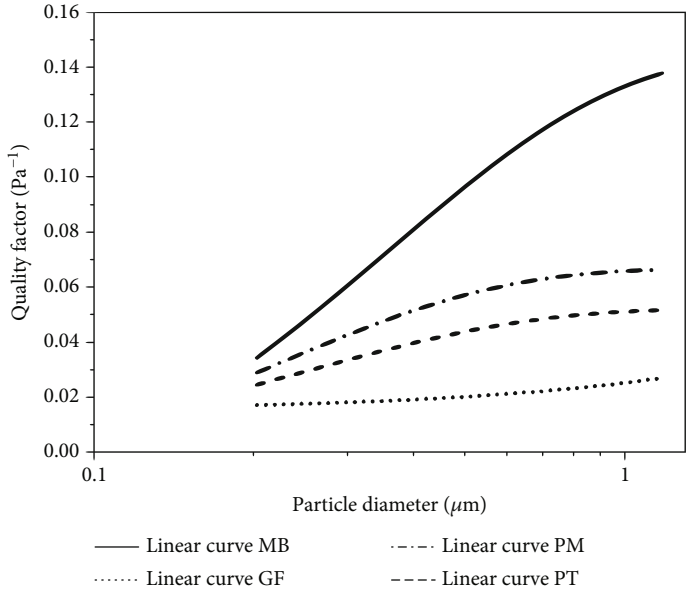

(a)

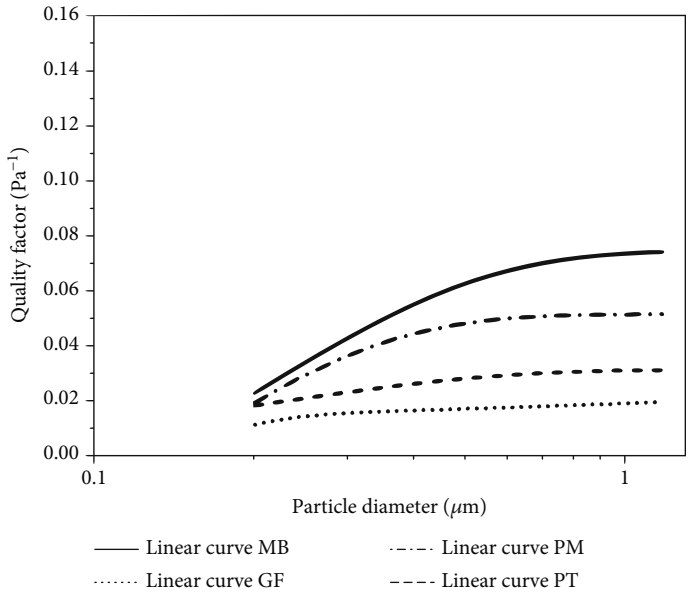

(b)

Figure 5: Continued.

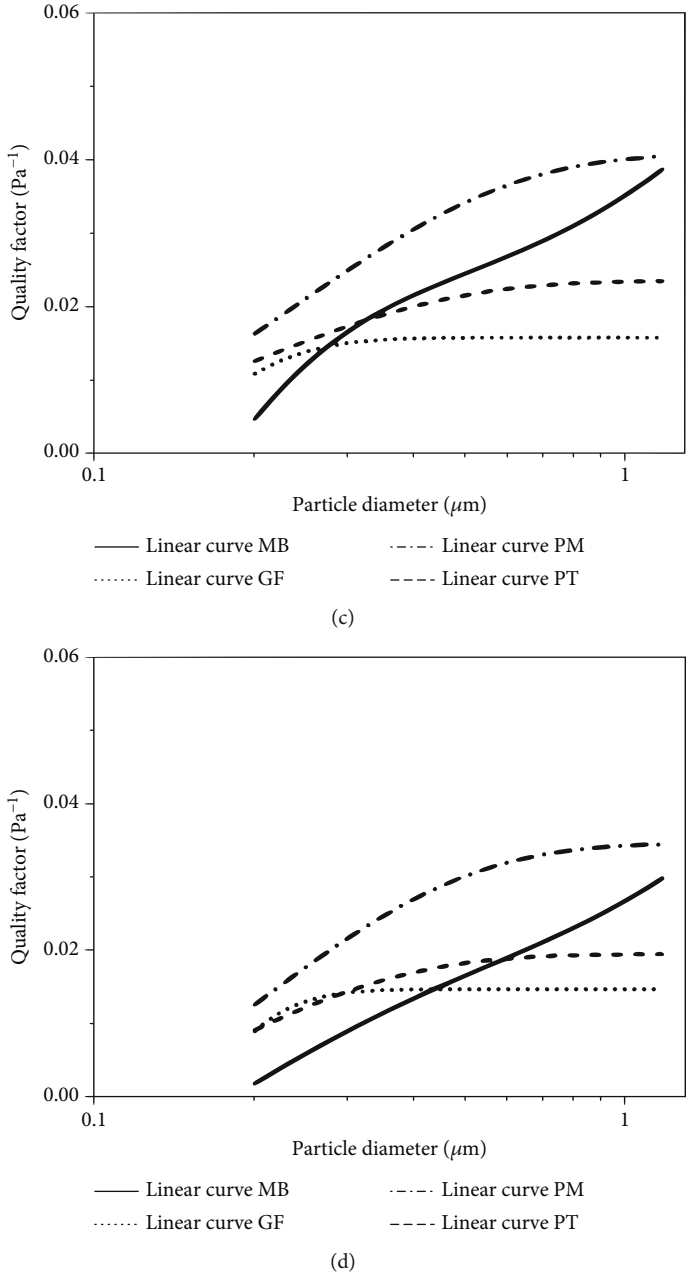

Figure 5: The performance of QF evaluated using the ExpDec2 model, which examines the changes in performance between the initial value and particle loading for various particle sizes in the melt-blown (MB), glass fiber (GF), PT + MB (PM), and PTFE membrane (PT) materials. (a) The initial cycle (without loading), (b) the second cycle, (c) the fourth cycle, and (d) the sixth cycle.

for GF, and 22.0% for PM (Figure 5(b)). The average QF values were higher in the order of PM, MB, PT, and GF, with the lowest QF value of 0.0079 Pa^{-1} for the MB filter in the range of 0.201–0.245 μm (Figure 5(c)). As a result, the QF value increased in the order of PM, PT, GF, and MB. The greatest change observed in the MB filter was 90.4% lower than the initial value in the range of 0.201–0.245 μm (Figure 5(d)).

3.3. Comparison of CADR for Different Particle Diameters. The CADR was standardized to a particle size of 0.3 μm in accordance with SPS-KACA002-132 standards, and the sCADR (0.02–0.113 μm) was also measured for comparison. The most penetrating particle size (MPPS) for each filter was estimated through a CADR experiment using various particle sizes. The MB and PM filters recorded the lowest CADR when the particle size was 0.0914 μm, whereas the GF and PT filters recorded low values at 0.1018 μm.

Before particles (0 cycles), the CADR for the MB filter, based on a particle size of 0.3 μm, reached a maximum of 4.83 m^3/min, and the sCADR was similar or lower. Under the same conditions, the GF filter had a CADR of 1.54 m^3/min, the PM filter had a CADR of 3.62 m^3/min, and the PT filter had a CADR of 3.22 m^3/min (Figure 6(a)). After

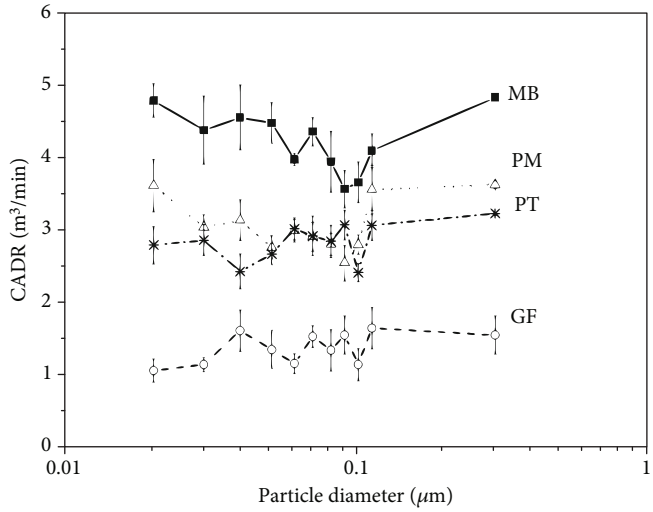

(a)

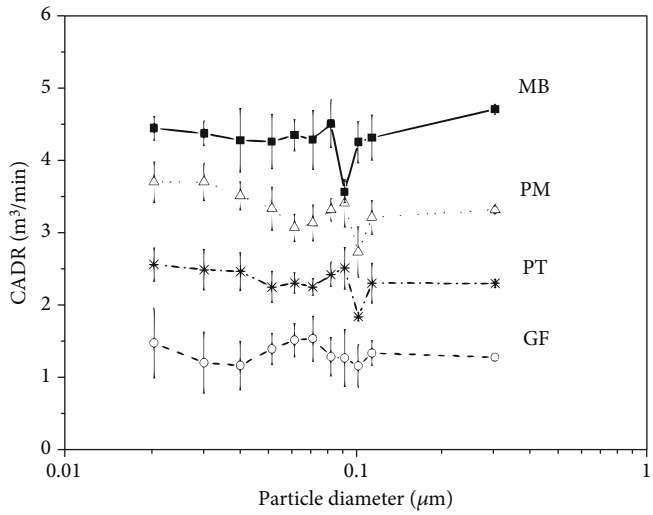

(b)

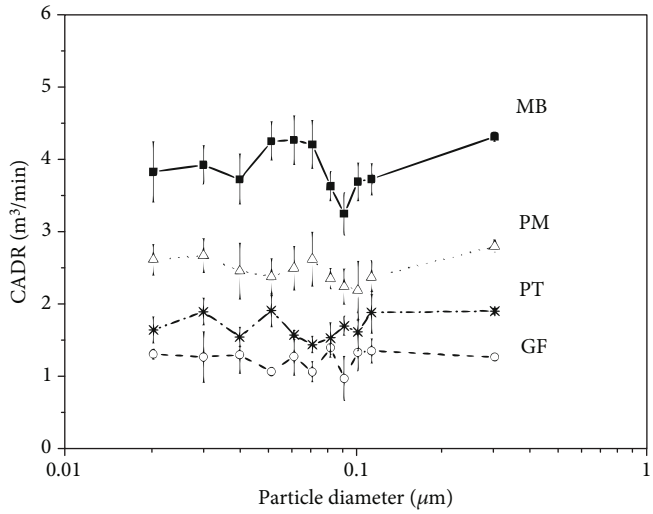

(c)

Figure 6: Continued.

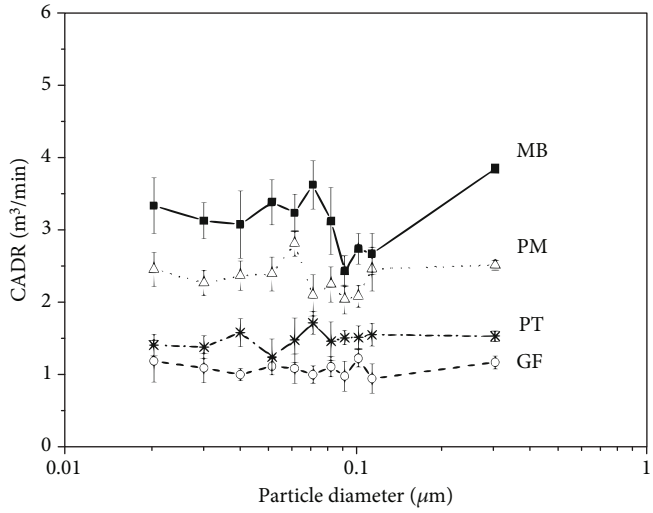

(d)

Figure 6: CADR performance of each filter depending on particle size and loading time: (a) the initial cycle (without loading), (b) the second cycle, (c) the fourth cycle, and (d) the sixth cycle. Data points represent the average of three repetitions, and error bars indicate standard deviations.

particle loading for two cycles, the CADR of the MB filter decreased by approximately 3.6% in comparison to the initial value, whereas the GF, PM, and PT filters decreased by 18.1%, 9.5%, and 29.5%, respectively (Figure 6(b)). The sCADR decreased similarly. After particle loading for four cycles, the PT filter showed the greatest drop of 41.2% compared to the initial value. The PM filter value decreased by 23.0%, whereas the GF and MB filters decreased by 18.4% and 10.9%, respectively (Figure 6(c)). After particle loading for six cycles, the performance of the MB filter decreased by 21.2% in comparison to the initial state, whereas the performance of the GF, PM, and PT filters decreased by 25.3%, 31.4%, and 53.1%, respectively (Figure 6(d)).

3.4. QF and CADR Values. The results of the regression analysis between QF and CADR are shown in Figure 7. The correlation was high for each filter type; however, the characteristics were different for each filter type. The slope of the linear equation for the MB filter was lower than that for the other filters. This is the case because the MB filter's QF decreased by 84%, and the air purifier's CADR decreased by 21.2% after particle loading. However, there was a high correlation coefficient ($r = 0.878$, $p < 0.0001$) between the QF and CADR for the MB filter. For the GF filter, the changes in the QF and CADR rates were 22.5% and 25.3%, respectively, and the correlation analysis showed a significant correlation ($r = 0.767$, $p < 0.05$) between QF and CADR. The slope of the PM filter was 48.82, a value between those of the MB and PT filters, and the correlation between the QF and CADR was high ($r = 0.958$, $p < 0.0001$). The QF change for the PT filter was approximately 55%, that for the CADR was 53.1%, and the correlation was high ($r = 0.962$, $p < 0.0001$).

3.5. CADR Performance after Particle Loading considering the Energy Efficiency of each Filter. The CADRs after particle loading, considering the energy efficiency of the air purifier, were altered (Figure 8). The CADR per 1 watt for the MB filter remained relatively stable at 0.144 m^3/min after six cycles of particle loading. However, the GF filter had the lowest initial CADR of 0.125 m^3/min·W and experienced the greatest decline of 33.3% (0.083 m^3/min·W) after six cycles of particle loading. The PM filter had the highest initial CADR of 0.151 m^3/min·W, which decreased by 8.3% (0.138 m^3/min·W) after particle loading. The PT filter had an initial CADR of 0.148 m^3/min·W, which dropped by 28.8% after particle loading.

4. Discussion

This study evaluated the performance of a researcher-designed PM filter in comparison to those of commonly utilized air purifier filters (MB, GF, and PT) by examining the changes in the initial capacity after particle loading. The objective was to determine the performance of the PM filter and its commercial viability.

Assessment of filter performance is generally based on two parameters: particle collection efficiency and pressure drop across the filter. The optimal filter offers the highest collection efficiency with the lowest pressure drop. Despite this, it is widely recognized that improving the collection efficiency of air filters leads to a corresponding increase in pressure drop [36, 37]. Consequently, the QF has become an invaluable tool for comparing the performance of different filters [38]. In this study, we conducted an initial measurement of the QF for each filter, followed by an analysis of the evolution of the QF for each particle size distribution as the particles accumulated on the filter.

The results showed that the initial performance order of MB > PM > PT > GF changed to the order of PM > PT > GF > MB after six cycles of loading. In this study, the QF values of various particle size distributions were measured

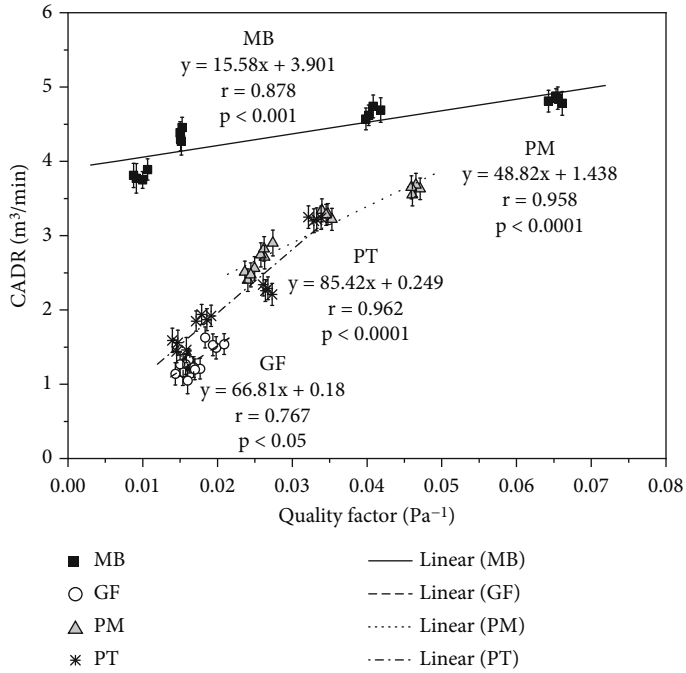

Figure 7: Performance correlation between QF values of filters and CADRs for the particle size of 0.3 μm: melt-blown (MB), glass fiber (GF), PTFE membrane (PT), and PT-MB combined media (PM). Data points represent the average of three repetitions, and error bars indicate standard deviations.

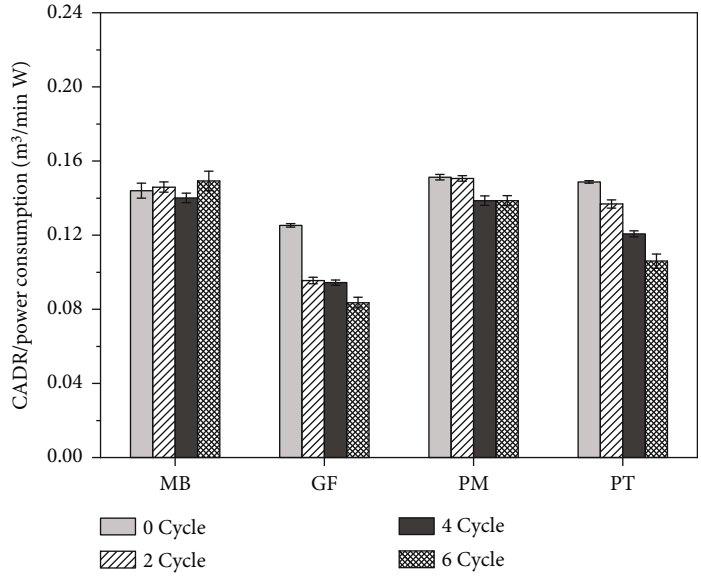

Figure 8: Changes in the CADR per consumption power for filters after particle loading: melt-blown (MB), glass fiber (GF), PTFE membrane (PT), and PT-MB combined media (PM).

for each filter. QF values between 0.201 and 0.245 μm were low for all filters, whereas QF values for the particle range of 0.835–1.17 μm were high because of the higher particle collection efficiency compared to the pressure drop. The reason for the low particle capture efficiency in the range of 0.201–0.245 μm is that this range is the MPPS range of the filter [36, 39]. The variation in QF value based on particle size distribution was consistent with previous research findings. Additionally, as reported in earlier studies, pleated filters demonstrated greater fluctuations in QF value in response to particle size distribution than flat filters, thereby supporting our current findings [40]. After particles were loaded onto the filters, QF values in the range of 0.201–0.245 μm were reduced, with a reduction of 90.4% for the MB filter. These findings align with the results of previous studies that suggest that the static electricity safety of MB filters is

dependent on the filter material and aerosol, which can impact the static energy and a potential threat to human safety [41, 42]. The GF filter demonstrated a depth filtration structure, leading to a slow increase in pressure drop, which is consistent with prior research suggesting that the GF filter has a higher holding capacity than other filters [3]. However, the low QF value of the GF filter can be attributed to its fiberglass composition of microfibers [43]. The PT filter showed a minimal impact on the penetration rate after particle loading, but the pressure drop increased by 124%, reflecting its low holding capacity [3]. In contrast, the PM filter exhibited both surface and depth filtration characteristics, effectively addressing the limitations of both the MB and PT filters. The analysis of the PM filter following particle loading indicated that there might be some benefits in terms of QF.

The performance of air filters is commonly evaluated using the QF value, but when assessing the purification ability of air purifiers, the CADR, which is expressed as the product of the airflow rate and particle removal efficiency, is the preferred metric [40, 44, 45]. There has been a paucity of studies comparing the CADR performance of filters made from developed media for the purpose of evaluating filter lifespan. The present study evaluated the CADR and sCADR of each filter type, and the results showed that the order of MB > PM > PT > GF was not altered before and after particle loading. This finding is in contrast with the QF results. This contrast can be explained by the findings of previous studies, which showed that CADR measures the rate at which fine particles are removed from an enclosed space and that the airflow rate has the greatest impact on CADR performance [45]. Therefore, the highest CADR results were obtained in the order of the lowest pressure drop for the filters. The MB filter obtained a higher CADR than the other filters, even after particle loading. This can be attributed to the electret filter method, which utilizes electrostatic attraction and has a lower initial pressure drop than other filters. Furthermore, the MB filter had a higher holding capacity because of the depth filtration method, resulting in a smaller increase in pressure drop even after loading [3, 46–50]. We suggest that the reason for the inferior CADR of the PM filter compared to that of the MB filter is that the initial pressure drop was approximately 2.4-fold greater than that of the MB filter because of the combined PTFE and MB materials. Although the dust collection efficiency of the MB filter fabric was projected to deteriorate rapidly and impact the CADR after six cycles of particle loading, the primary factor that affected the CADR performance was the pressure drop rather than the dust collection efficiency. Therefore, further investigations are necessary to minimize the initial pressure drop to the level of the MB filter.

Effective management of indoor air quality necessitates a meticulous selection of the most suitable filters tailored to specific indoor environments. Establishing appropriate criteria that align with the indoor setting becomes imperative to determine whether to prioritize filters with high initial performance or opt for those with lower initial performance but extended lifespans. Notably, variations in clean air delivery rate (CADR) attributed to different filter materials further underscore the importance of selecting filters tailored to the prevailing situation and environment. A pivotal representative criterion for filter selection involves cost-benefit analysis, considering both filter performance and expected lifespans. Additionally, in the context of optimizing filter selection, cost-reference particle filtering proves advantageous, leveraging sequential Monte Carlo (SMC) techniques to estimate the states of discrete-time dynamic random systems [51, 52]. However, such an analysis was not conducted in this study. Therefore, further research is needed to derive an optimal method for selecting suitable filters, enabling the resolution of dynamic optimization problems using state models such as sequential Monte Carlo and other models to account for cost, performance, and lifespan considerations.

The sCADR results were similar to the CADR results because the materials used in the experiments, including PTFE, GF, and MB, have the capacity to eliminate submicron particles through most particle removal mechanisms. However, the lowest CADR in the range of 0.08–0.09 μm was measured as a result of this experiment. Presently, the particle size range for CADR differs from one standard to another, but it typically is in the range of 0.15 to 0.3 μm, similar to the MPPS range of filters [36, 39]. This finding suggests that the MPPS range for the product may be distinct from that of the filter, necessitating further research into the new measurement range of CADR.

The correlation between the QF value and CADR was relatively high, but the slope varied depending on the filter's dust removal mechanism or material. Therefore, relying solely on the QF value may not accurately predict the air-purifying performance of an air purifier because the CADR result value, which is derived based on the filter material or filter specification, can have a different distribution than the QF value.

This study has some limitations. First, the media used were not optimized for the bending angle or filter media area based on its thickness or characteristics. Additionally, while manufacturing the filters, the performance of filters of different sizes was not compared when fixing the horizontal and vertical thickness standards of the filters. Furthermore, the experiment was limited to an air purifier with a CADR of 4.3CMM, so the performance change at high and low CADR could not be evaluated. During the QF evaluation, submicron-sized particles were not evaluated; therefore, a comparative evaluation with sCADR was not possible. Moreover, the filter's durability characteristics against KCl, NaCl, and diesel particles, other than the DEHS and A2 particles used for filter loading, could not be analyzed. Finally, the study was limited because the flow path structure of the product and the type of fan was not optimized based on the filter pressure drop.

5. Conclusion

In conclusion, meticulous filter selection is crucial for effective indoor air quality management. The newly developed PM filter shows promise in extending the filter lifespan while maintaining air purification efficacy. This suggests that it may serve as a substitute for the MB filter, which is used commercially but exhibits a rapid decline in particle collection efficiency after particle loading. Thus, if employed as an air purification device filter in medical institutions, childcare

centers, elderly care facilities, and other multiuse facilities requiring long-term indoor air quality management, the filter has the potential to maintain indoor air quality over an extended duration. However, its introduction may lead to a lower CADR, necessitating further research for CADR enhancement strategies. Future research should focus on optimizing filter design and performance to effectively address dynamic indoor air quality management challenges, underscoring the need for ongoing investigation in this area.

Data Availability

Data will be made available on request.

Conflicts of Interest

The authors declare no competing interests.

Authors' Contributions

H. Yun was responsible for the conceptualization, writing of the original draft, methodology, measurement, investigation, analysis, and visualization. J.H. Seo was responsible for the writing of the original draft, investigation, analysis, and funding acquisition. J. Yang was responsible for the conceptualization, review and editing of the original draft, and supervision. Hyunjun Yun and Ji Hoon Seo contributed equally to this work.

Acknowledgments

This research was supported by the Basic Science Research Program through the National Research Foundation of Korea (NRF) funded by the Ministry of Education (NRF-2021R1A6A3A01088686 and RS-2023-00244833) and Semyung University. This research was also supported by the "Particulate Matter Management Specialized Graduate Program" through the Korea Environmental Industry & Technology Institute (KEITI) funded by the Ministry of Environment (MOE).

Supplementary Materials

Table S1: parameters of the media tested in this study. Table S2: features of the tested air purifiers. Table S3: QF value for filter type. Figure S1: schematic of the test chamber specified in the KACA to evaluate the performance of a portable air purifier. Figure S2: comparison of filtration penetration and pressure drop of MB, GF, PM, and PT filters at particle size 0.3 μm and face velocity 1 m/s. *(Supplementary Materials)*

References

[1] D.-Q. Chang, S.-C. Chen, and D. Y. H. Pui, "Capture of sub-500 nm particles using residential electret HVAC filter media-experiments and modeling," *Aerosol and Air Quality Research*, vol. 16, no. 12, pp. 3349–3357, 2016.

[2] D. Y. H. Pui, S.-C. Chen, and Z. Zuo, "$PM_{2.5}$ in China: measurements, sources, visibility and health effects, and mitigation," *Particuology*, vol. 13, pp. 1–26, 2014.

[3] D.-Q. Chang, C.-Y. Tien, C.-Y. Peng, M. Tang, and S.-C. Chen, "Development of composite filters with high efficiency, low pressure drop, and high holding capacity $PM_{2.5}$ filtration," *Separation and Purification Technology*, vol. 212, pp. 699–708, 2019.

[4] R. L. Peck, S. A. Grinshpun, M. Yermakov, M. B. Rao, J. Kim, and T. Reponen, "Efficiency of portable HEPA air purifiers against traffic related combustion particles," *Building and Environment*, vol. 98, pp. 21–29, 2016.

[5] J. Liu, D. Y. H. Pui, and J. Wang, "Removal of airborne nanoparticles by membrane coated filters," *Science of the Total Environment*, vol. 409, no. 22, pp. 4868–4874, 2011.

[6] J. Wang, C. Asbach, H. Fissan et al., "How can nanobiotechnology oversight advance science and industry: examples from environmental, health, and safety studies of nanoparticles (nano-EHS)," *Journal of Nanoparticle Research*, vol. 13, no. 4, pp. 1373–1387, 2011.

[7] A. D. Maynard and D. Y. Pui, *Nanoparticles and Occupational Health*, vol. 186, Springer, 2007.

[8] R. Thakur, D. Das, and A. Das, "Electret air filters," *Separation & Purification Reviews*, vol. 42, no. 2, pp. 87–129, 2013.

[9] W. W.-F. Leung and Q. Sun, "Charged PVDF multilayer nanofiber filter in filtering simulated airborne novel coronavirus (COVID-19) using ambient nano-aerosols," *Separation and Purification Technology*, vol. 245, article 116887, 2020.

[10] R. I. Adams, M. Miletto, J. W. Taylor, and T. D. Bruns, "Dispersal in microbes: fungi in indoor air are dominated by outdoor air and show dispersal limitation at short distances," *The ISME Journal*, vol. 7, no. 7, pp. 1262–1273, 2013.

[11] T. A. Myatt, T. Minegishi, J. G. Allen, and D. L. MacIntosh, "Control of asthma triggers in indoor air with air cleaners: a modeling analysis," *Environmental Health*, vol. 7, no. 1, p. 43, 2008.

[12] K. H. Park, D. W. Sim, S. C. Lee et al., "Effects of air purifiers on patients with allergic rhinitis: a multicenter, randomized, double-blind, and placebo-controlled study," *Yonsei Medical Journal*, vol. 61, no. 8, pp. 689–697, 2020.

[13] R. J. Shaughnessy and R. G. Sextro, "What is an effective portable air cleaning device? A review," *Journal of Occupational and Environmental Hygiene*, vol. 3, no. 4, pp. 169–181, 2006.

[14] ANSI A, *AHAM Standard AC-1-2006, Method for Measuring Performance of Portable Household Electric Room Air Cleaners*, Association of Home Appliance Manufacturers, Washington, DC, 2006.

[15] GB, *GB/T18801: 2015 Air Cleaner Test Method*, Chineses Standard, 2015.

[16] KACA, *SPS-KACA002-132, Room Air Cleaning Device Standard*, Korea Air Cleaning Association (KACA), 2018.

[17] L. Du, S. Batterman, E. Parker et al., "Particle concentrations and effectiveness of free-standing air filters in bedrooms of children with asthma in Detroit, Michigan," *Building and Environment*, vol. 46, no. 11, pp. 2303–2313, 2011.

[18] M. S. Zuraimi, G. J. Nilsson, and R. J. Magee, "Removing indoor particles using portable air cleaners: implications for residential infection transmission," *Building and Environment*, vol. 46, no. 12, pp. 2512–2519, 2011.

[19] J. H. Ji, G. N. Bae, S. H. Kang, and J. Hwang, "Effect of particle loading on the collection performance of an electret cabin air filter for submicron aerosols," *Journal of Aerosol Science*, vol. 34, no. 11, pp. 1493–1504, 2003.

[20] D. C. Walsh and J. I. T. Stenhouse, "The effect of particle size, charge, and composition on the loading characteristics of an electrically active fibrous filter material," *Journal of Aerosol Science*, vol. 28, no. 2, pp. 307–321, 1997.

[21] R. C. Brown, D. Wake, R. Gray, D. B. Blackford, and G. J. Bostock, "Effect of industrial aerosols on the performance of electrically charged filter material," *The Annals of Occupational Hygiene*, vol. 32, no. 3, pp. 271–294, 1988.

[22] K. Sutherland, "Filtration overview: a closer look at depth filtration," *Filtration & Separation*, vol. 45, no. 8, pp. 25–28, 2008.

[23] N. Galka and A. Saxena, "High efficiency air filtration: the growing impact of membranes," *Filtration & Separation*, vol. 46, no. 4, pp. 22–25, 2009.

[24] Y.-M. Kuo, S.-H. Huang, W.-Y. Lin, M.-F. Hsiao, and C.-C. Chen, "Filtration and loading characteristics of granular bed filters," *Journal of Aerosol Science*, vol. 41, no. 2, pp. 223–229, 2010.

[25] T. Y. Ling, J. Wang, and D. Y. H. Pui, "Measurement of retention efficiency of filters against nanoparticles in liquids using an aerosolization technique," *Environmental Science & Technology*, vol. 44, no. 2, pp. 774–779, 2010.

[26] (NIOSH) NIfOSaH, *Respiratory protective devices. 42 CFR Part 84. Code of Federal Regulations*, US Government Printing Office, Office of the Federal Register, Washington, DC, 1995.

[27] S. Rengasamy, R. Shaffer, B. Williams, and S. Smit, "A comparison of facemask and respirator filtration test methods," *Journal of Occupational and Environmental Hygiene*, vol. 14, no. 2, pp. 92–103, 2017.

[28] S.-H. Huang, C.-W. Chen, Y.-M. Kuo, C.-Y. Lai, R. McKay, and C.-C. Chen, "Factors affecting filter penetration and quality factor of particulate respirators," *Aerosol and Air Quality Research*, vol. 13, no. 1, pp. 162–171, 2013.

[29] Organization IS, *Road vehicles—air filters for passenger compartments—part 1: test for particulate filtration*, International Electrotechnical Commission, Geneva, 2001.

[30] D. Ogulei, P. K. Hopke, and L. A. Wallace, "Analysis of indoor particle size distributions in an occupied townhouse using positive matrix factorization," *Indoor Air*, vol. 16, no. 3, pp. 204–215, 2006.

[31] L. Wallace, "Indoor sources of ultrafine and accumulation mode particles: size distributions, size-resolved concentrations, and source strengths," *Aerosol Science and Technology*, vol. 40, no. 5, pp. 348–360, 2006.

[32] T. Dziubak, "Experimental studies of powercore filters and pleated filter baffles," *Materials*, vol. 15, no. 20, p. 7292, 2022.

[33] Q. Zhang, J. Welch, H. Park, C.-Y. Wu, W. Sigmund, and J. C. M. Marijnissen, "Improvement in nanofiber filtration by multiple thin layers of nanofiber mats," *Journal of Aerosol Science*, vol. 41, no. 2, pp. 230–236, 2010.

[34] H. Yang, H. Zhu, and H. Fu, "Numerical calculation and analysis of filtration performance of an effective novel structural fiber for $PM_{2.5}$," *PLoS One*, vol. 15, no. 10, article e0240941, 2020.

[35] J. Wang, S. C. Kim, and D. Y. H. Pui, "Figure of merit of composite filters with micrometer and nanometer fibers," *Aerosol Science and Technology*, vol. 42, no. 9, pp. 722–728, 2008.

[36] D. Buivydiene, A. M. Todea, C. Asbach, E. Krugly, D. Martuzevicius, and L. Kliucininkas, "Composite micro/nano fibrous air filter by simultaneous melt and solution electrospinning," *Journal of Aerosol Science*, vol. 154, article 105754, 2021.

[37] Z. Wang, C. Zhao, and Z. Pan, "Porous bead-on-string poly (lactic acid) fibrous membranes for air filtration," *Journal of Colloid and Interface Science*, vol. 441, pp. 121–129, 2015.

[38] Y. H. Joe, K. Woo, and J. Hwang, "Fabrication of an anti-viral air filter with SiO_2–ag nanoparticles and performance evaluation in a continuous airflow condition," *Journal of Hazardous Materials*, vol. 280, pp. 356–363, 2014.

[39] Q. Sun and W. W.-F. Leung, "Charged PVDF multi-layer filters with enhanced filtration performance for filtering nanoaerosols," *Separation and Purification Technology*, vol. 212, pp. 854–876, 2019.

[40] Y. L. Kim, M. S. Kwon, and M. H. Lee, "Optimized pleat geometry at specific pleat height in pleated filters for air purification," *Indoor Air*, vol. 32, no. 10, Article ID e13135, 2022.

[41] A. Brochocka, K. Makowski, and K. Majchrzycka, "Penetration of different nanoparticles through melt-blown filter media used for respiratory protective devices," *Textile Research Journal*, vol. 82, no. 18, pp. 1906–1919, 2012.

[42] T.-C. Hsiao and D.-R. Chen, "Experimental observations of the transition pressure drop characteristics of fibrous filters loaded with oil-coated particles," *Separation and Purification Technology*, vol. 149, pp. 47–54, 2015.

[43] Z.-J. Zhou, B. Zhou, C.-H. Tseng, S.-C. Hu, A. Shiue, and G. Leggett, "Evaluation of characterization and filtration performance of air cleaner materials," *International Journal of Environmental Science and Technology*, vol. 18, no. 8, pp. 2209–2220, 2021.

[44] K.-C. Noh and M.-D. Oh, "Variation of clean air delivery rate and effective air cleaning ratio of room air cleaning devices," *Building and Environment*, vol. 84, pp. 44–49, 2015.

[45] J. S. Kim and M. H. Lee, "Effect of filter collection efficiency on the clean air delivery rate in an air cleaner," *Indoor Air*, vol. 31, no. 3, pp. 745–754, 2021.

[46] M. Lee, Y. Otani, N. Namiki, and H. Emi, "Prediction of collection efficiency of high-performance electret filters," *Journal of Chemical Engineering of Japan*, vol. 35, no. 1, pp. 57–62, 2002.

[47] S.-M. Ji, J.-R. Sohn, and H.-S. Park, "Influence of particle and filter charge on filtration property of air filter under particle loading," *Journal of Korean Society for Atmospheric Environment*, vol. 28, no. 6, pp. 644–655, 2012.

[48] H.-J. Choi, S. B. Kim, S. H. Kim, and M.-H. Lee, "Preparation of electrospun polyurethane filter media and their collection mechanisms for ultrafine particles," *Journal of the Air & Waste Management Association*, vol. 64, no. 3, pp. 322–329, 2014.

[49] M. Kerner, K. Schmidt, S. Schumacher, V. Puderbach, C. Asbach, and S. Antonyuk, "Evaluation of electrostatic properties of electret filters for aerosol deposition," *Separation and Purification Technology*, vol. 239, article 116548, 2020.

[50] W. J. Lee, H. B. Kim, H. Eom, J. Hwang, and M. H. Lee, "Effect of surface charge density on electret filters charge degradation by organic solvent exposure," *Environmental Engineering Research*, vol. 28, no. 1, article 210523, 2023.

[51] L. Martino, J. Read, V. Elvira, and F. Louzada, "Cooperative parallel particle filters for online model selection and applications to urban mobility," *Digital Signal Processing*, vol. 60, pp. 172–185, 2017.

[52] J. Míguez, "Analysis of selection methods for cost-reference particle filtering with applications to maneuvering target tracking and dynamic optimization," *Digital Signal Processing*, vol. 17, no. 4, pp. 787–807, 2007.